

Synthesis of Au(Core)/Ag(Shell) Nanoparticles and their Conversion to AuAg Alloy Nanoparticles

Matthew S. Shore, Junwei Wang, Aaron C. Johnston-Peck, Amy L. Oldenburg, and Joseph B. Tracy*

Metal nanoparticles (NPs) are of great interest due to their special optical,^[1–3] electronic,^[4–8] and catalytic^[9,10] properties.^[11] Among metal NPs, Au NPs have been investigated most extensively because of their facile preparation, resistance to oxidation, and surface plasmon resonance (SPR) band that can absorb and scatter visible light.^[3] Core/shell and alloy bimetallic NPs are especially interesting because they provide opportunities to tune the NPs' optical and catalytic properties^[12–15] and are potentially useful as taggants for security applications.^[2] The AuAg system is of particular interest because the SPR band is tunable between ~520 nm for Au^[11] and ~410 nm for Ag.^[16] Several syntheses for AuAg alloy,^[15,17–37] Au(core)/Ag(shell),^[22,25,31,33,35–45] and Ag(core)/Au(shell) NPs^[28,31,33–35,42,46–48] have already been reported.

Here, we report a facile, stoichiometrically controlled synthesis of Au(core)/Ag(shell) and AuAg alloy NPs through digestive ripening,^[49–51] which is a potentially general method for synthesizing alloy NPs.^[37,52,53] Au(core)/Ag(shell) NPs were synthesized and annealed to form AuAg alloy NPs, followed by elemental analysis and structural and optical characterization. Methods utilizing Au rather than Ag NPs as the seed particles are advantageous: obtaining monodisperse Ag NPs is significantly more challenging^[16] because it is harder to control the nucleation of Ag NPs and to avoid oxidation. Huang and co-workers recently demonstrated the conversion of Au(core)/Ag(shell) to AuAg alloy NPs as a part of a larger study showing the generality of digestive ripening for synthesizing alloy NPs, but very limited data without quantitative elemental analysis or optical characterization of the AuAg alloy NPs was provided.^[37] In this study, we compare a two-step synthesis of Au(core)/Ag(shell) NPs and their conversion to AuAg alloy NPs through annealing with a one-step, direct conversion of Au NPs to AuAg alloy NPs. The products of

the one-step reaction have the same Au:Ag stoichiometry as the reactants, thus giving quantitative control.

This report is closely related to two recent studies by the group of S. H. Sun: in one study, amine-stabilized Ag(core)/Au(shell) NPs were synthesized and then annealed to form AuAg alloy NPs.^[34] In another study, AuAg alloy NPs were synthesized through simultaneous reduction of gold and silver salts.^[15] In our two-step method, amine-stabilized Au NPs were first prepared through digestive ripening using dodecylamine (DDA) in refluxing toluene under inert atmosphere to improve their monodispersity.^[54,55] A solution of silver acetate (AgOAc) dissolved in toluene and DDA was then added, and refluxing was continued for growing the Ag shells. The amount of AgOAc added controlled the stoichiometry of the Au(core)/Ag(shell) NPs. The Au(core)/Ag(shell) NPs were then isolated and annealed in oleylamine (OLA) at 250 °C for transformation to AuAg alloy NPs. The one-step method skips the Au(core)/Ag(shell) structure by transferring the Au seeds to a solution of AgOAc in OLA and annealing at 250 °C. The SPR absorbance of the alloys can be tuned by adjusting the Au:Ag molar ratio of the precursors, which controls the composition. These alloys may also have potentially useful catalytic properties, and amines can be removed more easily than thiols, which are permanent catalyst poisons and were not used in this synthesis.

Other amine chain lengths for ripening and growth of the Ag shells were explored, but shorter chains caused irreversible precipitation during growth of the Ag shells, and longer chain lengths greatly slowed the rate of Ag shell growth; DDA provided solubility and reasonable growth rates. Amines are known to serve as reducing agents at elevated temperatures,^[56–59] and DDA reduces the Ag(I)–DDA complexes to Ag(0). We note that growth of Ag shells on Au cores requires a reducing agent for reducing Ag(I) to Ag(0). In contrast, growth of Au shells on Ag can often be accomplished by galvanic exchange or transmetalation reactions that oxidize Ag(0) to Ag(I) dissolved in solution while reducing Au(III) or Au(I) to Au(0). In the galvanic exchange approach, it can be challenging to control the etching of the Ag core. OLA was chosen for the annealing step because it maintained NP solubility at elevated temperatures; when using shorter-chained amines, the NPs precipitated before annealing could be completed.

NP size measurements from transmission electron microscopy (TEM) (**Figure 1** and Figure S1, Supporting Information) and optical absorbance spectra (**Figure 2** and Figures S7–S9,

M. S. Shore, Dr. J. Wang, A. C. Johnston-Peck, Prof. J. B. Tracy
Department of Materials Science and Engineering
North Carolina State University
Raleigh, NC 27695, USA
E-mail: jbttracy@ncsu.edu
Prof. A. L. Oldenburg
Department of Physics and Astronomy
University of North Carolina
Chapel Hill, NC 27599, USA

DOI: 10.1002/sml.201001138

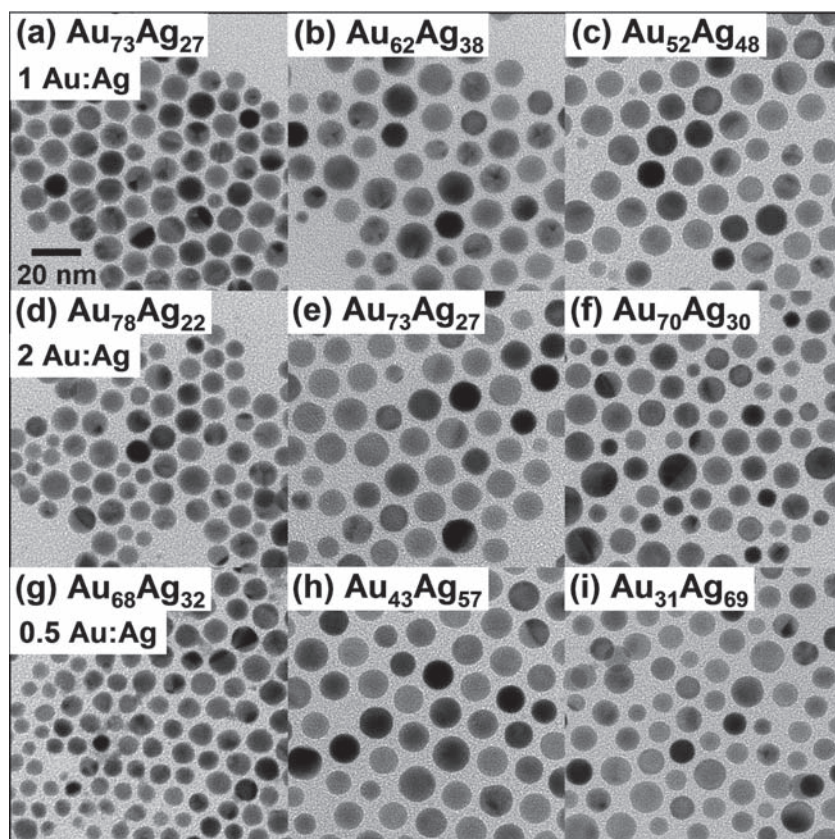


Figure 1. TEM of bimetallic AuAg nanoparticles using different Au:Ag molar ratios in the precursors: 1:1 (a–c), 2:1 (d–f), and 0.5:1 (g–i). Au(core)/Ag(shell) (a,d,g) and AuAg alloy nanoparticles (b,e,h) were synthesized following the two-step method and were compared with AuAg alloy nanoparticles synthesized using the one-step method (c,f,i). The composition of each sample measured by EDS is indicated.

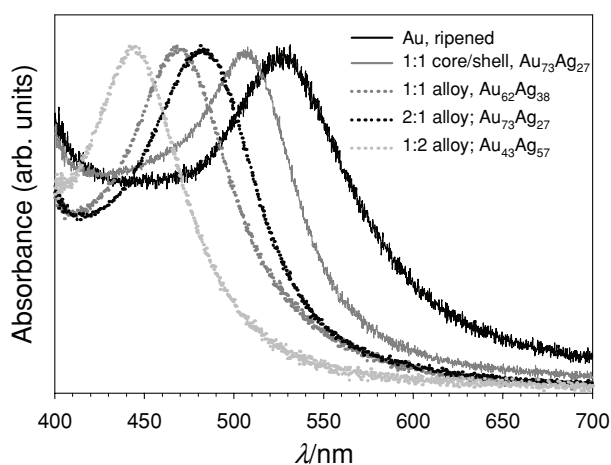


Figure 2. Normalized absorbance spectra for Au and AuAg alloy nanoparticles synthesized through the two-step method using different Au:Ag precursor molar ratios.

Supporting Information) were acquired for the Au NPs after ripening and after further ripening with various amounts of AgOAc to form Au(core)/Ag(shell) NPs and alloy NPs (Table 1). The composition of each sample is specified by two quantities, the Au:Ag molar ratio in the precursors, and the

composition ($\text{Au}_x\text{Ag}_{100-x}$) of the purified product measured by energy dispersive X-Ray spectroscopy (EDS, Figure S-6, Supporting Information). From the EDS measurements, the typical relative standard error of the Au:Ag molar ratio was 7%, which propagated into a standard error in the compositions, $\text{Au}_{x\pm\sigma}\text{Ag}_{(100-x)\pm\sigma}$, of $\sigma = 1.5$.

TEM (Figure 1) and high-resolution TEM (HRTEM) (Figures S2–S5, Supporting Information) images show nanostructural changes that are consistent with the growth of Ag shells followed by alloying. In several TEM images, the shells can be partially distinguished from the cores (Figure 1a,d,g) because the lower atomic number of Ag provides less contrast in TEM than Au. The boundary between the core and shell is not sharp, however, which suggests that the shells might be AuAg alloys rather than pure Ag. If the shells are AuAg alloys, the composition is likely graded, so that they are the most Ag-rich on the NP surface. Graded shells would arise from a kinetically controlled process that has not gone to completion, and there is more thermodynamic driving force for Ag on the surface rather than Au.^[31] As expected, the contrast becomes uniform upon alloying. The Au, Ag, and AuAg phases are nearly isomorphous, which prevents the use of diffraction methods for distinguishing between the different phases. We have not

been able to obtain useful measurements by Z-contrast TEM due to contamination from the organic ligands.

We further note that the size measurements by TEM indicate that conversion of Au(core)/Ag(shell) NPs to alloy NPs involves ripening (i.e., interparticle transfer of metal atoms). The alloy NPs have significantly larger sizes than the core/shell NPs, which can only be explained by ripening. The interparticle spacing (Figure 1) also increases during alloying, when DDA ligands are replaced with OLA. HRTEM images show that alloying also reduces the number of crystal defects in the NPs (Figures S2–S4, Supporting Information).

Elemental analysis by EDS elucidates several important aspects of the shell growth and alloying mechanism: we note that all of the Au(core)/Ag(shell) NPs have similar compositions ($X_{\text{Ag}} = 0.22\text{--}0.32$), despite a fourfold variation in the amount of AgOAc used in the synthesis. Within this range of compositions, the core/shell NPs can be synthesized with stoichiometric control, but the reactant molar ratio must be enriched in Ag to achieve a target product composition. As deposition of Ag proceeds, further deposition of Ag becomes less energetically favorable, which implies a practical upper limit to the amount of Ag incorporated in the shell. We are unsure of the origin of this limiting behavior; it might arise from differences in the amine ligand binding to Au and Ag, oxidation of the Ag shell, or possibly from electronic charging

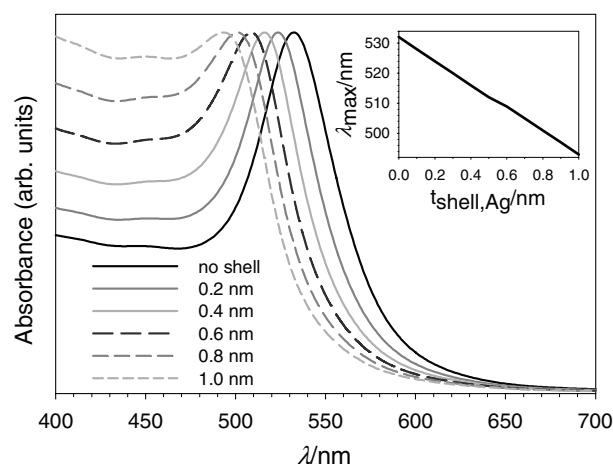
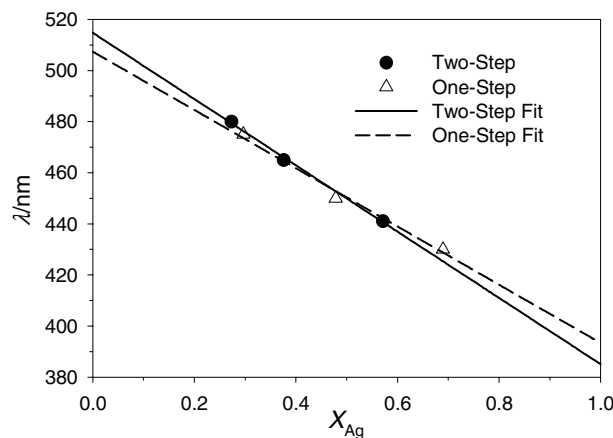
Table 1. Summary of results for AuAg core/shell and alloy nanoparticles: elemental analysis (EDS), UV-vis spectroscopy, and size analysis (TEM).

Method	Structure	Au:Ag precursor molar ratio	Au:Ag product molar ratio	Product composition	Absorbance maximum [nm]	d_{core} [nm]
control	Au core	–	–	Au	528	8.0 ± 0.9
two-step	core/shell	1:1	2.73	$\text{Au}_{73}\text{Ag}_{27}$	507	9.8 ± 1.4
two-step	alloy	1:1	1.66	$\text{Au}_{62}\text{Ag}_{38}$	465	10.8 ± 2.1
two-step	core/shell	2:1	3.57	$\text{Au}_{78}\text{Ag}_{22}$	515	9.3 ± 1.6
two-step	alloy	2:1	2.66	$\text{Au}_{73}\text{Ag}_{27}$	480	10.8 ± 1.8
two-step	core/shell	1:2	2.10	$\text{Au}_{68}\text{Ag}_{32}$	515	8.5 ± 1.2
two-step	alloy	1:2	0.75	$\text{Au}_{43}\text{Ag}_{57}$	441	11.1 ± 1.8
one-step	alloy	1:1	1.09	$\text{Au}_{52}\text{Ag}_{48}$	450	11.2 ± 1.9
one-step	alloy	2:1	2.37	$\text{Au}_{70}\text{Ag}_{30}$	475	11.4 ± 2.9
one-step	alloy	1:2	0.45	$\text{Au}_{31}\text{Ag}_{69}$	430	10.6 ± 1.8

during shell growth. After the growth of Au(core)/Ag(shell) NPs, some of the Ag precursor remains unreacted in the growth solution and is removed through the purification step before the transfer to OLA for annealing and conversion to alloy NPs. Upon annealing, the composition of the alloys is enriched in Ag despite no further addition of metal-containing reagents, which implies that some of the Au from the cores preferentially dissolves into OLA during alloying. The dependence of the core/shell and alloy NP composition on the reactant molar ratio is nearly linear and is plotted in Figure S10 (Supporting Information), which could be used for stoichiometric control. As a simplification of the two-step core/shell NP synthesis and alloying, we devised a one-step method for synthesizing the AuAg alloy NPs that anneals the Au NPs with AgOAc in OLA. An important advantage of the one-step method is that the Au:Ag molar ratio of the alloys is the same as the molar ratio of the reactants.

Formation of the Ag shells shifts the SPR absorbance from 528 nm for the Au seed NPs to 505–515 nm for the Au(core)/Ag(shell) NP (Figure 2 and Figure S8, Supporting Information). This shifted, single SPR absorbance band indicates coupling between the Au and Ag layers and is consistent with Au cores covered with Ag or AuAg alloy shells.^[35,46] Simulations of Au(core)/Ag(shell) NPs from Mie theory (Figure 3) match the experimental results well for shell thicknesses of ~0.5 nm and show the same blueshifted SPR absorbance band. We further note that the Au(core)/Ag(shell) NPs still show the increased baseline near 450 nm that arises from the interband transition of Au in the core.^[60]

Annealing the Au(core)/Ag(shell) NPs gave rise to greater blueshifts and sharpening of the SPR absorbance peaks, which indicates homogeneity and alloying. The linearity of the graphs of the peak of the SPR absorbance as a function of the Ag mole fraction (Figure 4) confirms alloying, as has also been reported for several other studies of AuAg alloy NPs.^[20,27,29,61] The narrow SPR absorbance bands (Figure 2 and Figure S9, Supporting Information) indicate uniform compositions throughout each sample. As the Ag composition in the AuAg alloy NPs increases, the SPR band sharpens because the magnitude of the

**Figure 3.** Normalized simulated absorbance spectra from Mie theory for 8.0 nm diameter Au nanoparticles with Ag shell thicknesses up to 1.0 nm dispersed in toluene. The inset shows the wavelength of the absorbance peak plotted versus the Ag shell thickness.**Figure 4.** Peak surface plasmon resonance absorbance wavelength plotted versus Ag mole fraction for the AuAg alloy nanoparticles.

imaginary part of the dielectric constant (ϵ_2) for Ag is substantially less than for Au in the visible spectrum,^[62] which reduces damping of the SPR.^[63] Conversion to the alloy requires heating to a higher temperature of 200–250 °C (Figure S7, Supporting Information) than was reported for converting Ag(core)/Au(shell) NPs to alloys by Sun and co-workers.^[34] This difference in annealing temperatures for alloying might be related to the greater nobility of Au than Ag.

The annealing process was devised by performing annealing at several temperatures and monitoring the SPR absorbance to find the minimum temperature that resulted in formation of the alloy in 20 min (Figure S7, Supporting Information). Heating to 200 °C was required to initiate alloying and to begin shifting the SPR absorbance band towards that of pure Ag. At 200 °C, the absorbance shows a broad shoulder that represents an inhomogeneous distribution of NPs with different extents of annealing. An annealing temperature of 250 °C was chosen because a single SPR absorbance band for the alloy emerged. An annealing time of 2 h was chosen to ensure complete alloying.

In conclusion, we have developed a facile synthesis of Au(core)/Ag(shell) NPs through the seeded growth of Ag onto Au NP seeds using digestive ripening followed by annealing, which causes their conversion to AuAg alloy NPs. This digestive ripening approach is general and potentially useful for synthesizing other kinds of core/shell and alloy NPs. We have shown quantitative control over the composition of the core/shell and alloy NPs, which allows tuning of the SPR absorbance and might enable tuning of their catalytic properties.

Experimental Section

Synthesis of Au Nanoparticles: The synthesis of Au NPs follows a method first developed by Klabunde and co-workers:^[5] Didodecyldimethylammonium bromide (93 mg, 0.20 mmol, 98%, TCI America) was dissolved in toluene (10 mL). While stirring, AuCl₃ (36 mg, 0.12 mmol, 64.4% Au, Alfa Aesar) was added, after which the mixture was sonicated for 10 s and turned a dark red-orange color before resuming stirring and sealing the flask with a septum to prevent evaporation. A solution of NaBH₄ (71 mg, 1.9 mmol, 98%, J. T. Baker) was prepared in distilled water (200 μ L) at room temperature, and 36 μ L of this solution was added dropwise to the mixture under vigorous stirring. While stirring for another 25 min, the color gradually changed until it became dark red-violet. DDA (0.82 mL, 3.6 mmol, 98+%, Alfa Aesar) was then added dropwise, and the solution was stirred for an additional 15 min. The NPs were then isolated by adding methanol and ethanol (200 proof) and centrifuging. After discarding the supernatant, the solids were redispersed in toluene (15 mL).

Preparation of Silver Acetate Solution: Silver acetate (AgOAc, 99%, Alfa Aesar) was dissolved in a mixture of toluene (7 mL) and DDA (0.30 mL, 1.3 mmol). The amount of AgOAc was adjusted to obtain the desired Au:Ag molar ratio. For molar ratios of 1:1, 1:2, and 2:1, amounts of 20, 40, and 10 mg of AgOAc were used respectively.

Two-Step Method: Au(Core)/Ag(Shell) Nanoparticles: The solution of Au NPs in toluene (15 mL) and additional DDA (0.82 mL, 3.6 mmol) were combined in a round-bottom flask. The mixture was refluxed at 120 °C under vigorous stirring and while bubbling nitrogen through the solution for 90 min. After this first ripening step, the entire AgOAc solution (giving the appropriate 1:1, 1:2, or 2:1 Au:Ag molar ratio) was added to the solution of Au NPs. The solution was refluxed for an additional 90 min with continued stirring under inert atmosphere. After cooling the product, it was divided into aliquots of ~5 mL. Each aliquot was centrifuged after adding methanol (7.5 mL) and ethanol (2.5 mL) to flocculate the NPs. Each aliquot of the Au(core)/Ag(shell) NP product could be redispersed in toluene for storage or in OLA (4.0 mL, 97%, Pfaltz & Bauer) for alloying.

Two-Step Method: AuAg Alloy Nanoparticles by Annealing Au(Core)/Ag(Shell) Nanoparticles: The fractions of the Au(core)/Ag(shell) NPs in OLA were combined and stirred in a flask that was then evacuated for one hour at room temperature before backfilling with nitrogen. The temperature was then quickly ramped (~15 °C min⁻¹) to 250 °C and held at this temperature for 2 h. After cooling to room temperature, the product was purified by adding a mixture of ethanol and methanol to flocculate the NPs, discarding the supernatant, and redispersing the NPs in toluene.

One-Step Method for AuAg Alloy Nanoparticles: The same methods for synthesizing and ripening Au NPs were carried out as described above. After ripening and purification, the Au NPs were redispersed in OLA (18.0 mL). For Au:Ag molar ratios of 1:1, 1:2, and 2:1, respective amounts of 20, 40, and 10 mg of AgOAc were dispersed in 8.0 mL OLA and added to the NPs. The mixture was evacuated for 1 h at room temperature before backfilling with nitrogen. The temperature was then quickly ramped (~15 °C min⁻¹) to 250 °C and held at this temperature for 2 h. Purification of the product was the same as for the two-step alloy NPs.

Characterization: The NPs were characterized using UV–vis absorbance spectroscopy (Ocean Optics CHEMUSB4-VIS-NIR spectrophotometer), TEM, HRTEM, and EDS. Absorbance measurements used toluene as the solvent. TEM images and EDS spectra were acquired using a JEOL 2000FX microscope, and HRTEM was performed using a JEOL 2010F microscope. The NP sizes were measured using publicly available ImageJ software.^[64] For each NP sample, the diameter and standard deviation were determined by averaging measurements of 100 NPs. The Au:Ag composition was measured by EDS and quantified using the Cliff–Lorimer method. For calibrating the EDS measurements, one of the bimetallic AuAg samples was submitted to Gailbraith Laboratories for analysis by inductively coupled plasma optical emission spectroscopy (ICP-OES).

Simulated Absorbance Spectra for Au(Core)/Ag(Shell) Nanoparticles: Mie theory calculations were employed for simulating the absorbance spectra of coated spheres according to the methods of Bohren and Huffman.^[65] The complex refractive indices of Au and Ag^[62] and the real refractive index of toluene^[66] were spline interpolated over the 400–700 nm wavelength range with a 1 nm step size. Calculations of the extinction efficiency, which is proportional to absorbance, were performed for Au cores of 8.0 nm diameter, with Ag shell thicknesses stepped from 0 to 1.0 nm in 0.1 nm increments, in a toluene medium.

Supporting Information

Supporting Information is available from the Wiley Online Library or from the author.

Acknowledgements

This work was supported by the National Science Foundation (CHE-0943975) and startup funds from North Carolina State University. We thank Emilie Ringe for helpful discussions and Tom Rawdanowicz for assistance with TEM.

- [1] S. Link, M. A. El-Sayed, *J. Phys. Chem. B* **1999**, *103*, 8410.
- [2] J. P. Wilcoxon, B. L. Abrams, *Chem. Soc. Rev.* **2006**, *35*, 1162.
- [3] P. K. Jain, K. S. Lee, I. H. El-Sayed, M. A. El-Sayed, *J. Phys. Chem. B* **2006**, *110*, 7238.
- [4] U. Simon, *Adv. Mater.* **1998**, *10*, 1487.
- [5] J. Wang, *Anal. Chim. Acta* **2003**, *500*, 247.
- [6] N. J. Yang, K. Aoki, H. Nagasawa, *J. Phys. Chem. B* **2004**, *108*, 15027.

- [7] B. E. Brinson, J. B. Lassiter, C. S. Levin, R. Bardhan, N. Mirin, N. J. Halas, *Langmuir* **2008**, *24*, 14166.
- [8] A. V. Moskalenko, S. N. Gordeev, O. F. Koentjoro, P. R. Raithby, R. W. French, F. Marken, S. E. Savel'ev, *Phys. Rev. B* **2009**, *79*, 241403(R).
- [9] M. S. Chen, D. W. Goodman, *Acc. Chem. Res.* **2006**, *39*, 739.
- [10] G. C. Bond, D. T. Thompson, *Catal. Rev. – Sci. Eng.* **1999**, *41*, 319.
- [11] M. C. Daniel, D. Astruc, *Chem. Rev.* **2004**, *104*, 293.
- [12] A. Q. Wang, C. M. Chang, C. Y. Mou, *J. Phys. Chem. B* **2005**, *109*, 18860.
- [13] A. Q. Wang, J. H. Liu, S. D. Lin, T. S. Lin, C. Y. Mou, *J. Catal.* **2005**, *233*, 186.
- [14] X. Y. Liu, A. Q. Wang, X. D. Wang, C. Y. Mou, T. Zhang, *Chem. Commun.* **2008**, 3187.
- [15] C. Wang, H. G. Yin, R. Chan, S. Peng, S. Dai, S. H. Sun, *Chem. Mater.* **2009**, *21*, 433.
- [16] R. M. Bright, M. D. Musick, M. J. Natan, *Langmuir* **1998**, *14*, 5695.
- [17] P. Mulvaney, M. Giersig, A. Henglein, *J. Phys. Chem.* **1993**, *97*, 7061.
- [18] M. J. Hostetler, C. J. Zhong, B. K. H. Yen, J. Andereg, S. M. Gross, N. D. Evans, M. Porter, R. W. Murray, *J. Am. Chem. Soc.* **1998**, *120*, 9396.
- [19] S. Link, Z. L. Wang, M. A. El-Sayed, *J. Phys. Chem. B* **1999**, *103*, 3529.
- [20] Y. H. Chen, C. S. Yeh, *Chem. Commun.* **2001**, 371.
- [21] M. P. Mallin, C. J. Murphy, *Nano Lett.* **2002**, *2*, 1235.
- [22] T. Shibata, B. A. Bunker, Z. Y. Zhang, D. Meisel, C. F. Vardeman, J. D. Gezelter, *J. Am. Chem. Soc.* **2002**, *124*, 11989.
- [23] N. N. Kariuki, J. Luo, M. M. Maye, S. A. Hassan, T. Menard, H. R. Naslund, Y. H. Lin, C. M. Wang, M. H. Engelhard, C. J. Zhong, *Langmuir* **2004**, *20*, 11240.
- [24] Y. C. Liu, H. T. Lee, H. H. Peng, *Chem. Phys. Lett.* **2004**, *400*, 436.
- [25] O. M. Wilson, R. W. J. Scott, J. C. Garcia-Martinez, R. M. Crooks, *J. Am. Chem. Soc.* **2005**, *127*, 1015.
- [26] H. Z. Yin, X. W. He, H. Liu, W. Y. Li, L. X. Chen, *Chin. J. Anal. Chem.* **2005**, *33*, 939.
- [27] R. J. Chimentão, I. Cota, A. Dafinov, F. Medina, J. E. Sueiras, J. L. G. de la Fuente, J. L. G. Fierro, Y. Cesteros, P. Salagre, *J. Mater. Res.* **2006**, *21*, 105.
- [28] H. M. Chen, R. S. Liu, L. Y. Jang, J. F. Lee, S. F. Hu, *Chem. Phys. Lett.* **2006**, *421*, 118.
- [29] M. Zhou, S. H. Chen, S. Y. Zhao, H. Y. Ma, *Physica E* **2006**, *33*, 28.
- [30] P. Raveendran, J. Fu, S. L. Wallen, *Green Chem.* **2006**, *8*, 34.
- [31] Z. Y. Li, J. P. Wilcoxon, F. Yin, Y. Chen, R. E. Palmer, R. L. Johnston, *Faraday Discuss.* **2008**, *138*, 363.
- [32] W. X. Wang, Y. P. Huang, Q. F. Chen, S. K. Xu, D. Z. Yang, *Spectrosc. Spectral Anal.* **2008**, *28*, 1726.
- [33] F. Hubenthal, N. Borg, F. Träger, *Appl. Phys. B: Lasers Opt.* **2008**, *93*, 39.
- [34] C. Wang, S. Peng, R. Chan, S. H. Sun, *Small* **2009**, *5*, 567.
- [35] J. Wilcoxon, *J. Phys. Chem. B* **2009**, *113*, 2647.
- [36] C. M. Gonzalez, Y. Liu, J. C. Scaiano, *J. Phys. Chem. C* **2009**, *113*, 11861.
- [37] Y. Yang, X. Z. Gong, H. M. Zeng, L. J. Zhang, X. H. Zhang, C. Zou, S. M. Huang, *J. Phys. Chem. C* **2010**, *114*, 256.
- [38] R. G. Freeman, M. B. Hommer, K. C. Grabar, M. A. Jackson, M. J. Natan, *J. Phys. Chem.* **1996**, *100*, 718.
- [39] J. H. Hodak, A. Henglein, M. Giersig, G. V. Hartland, *J. Phys. Chem. B* **2000**, *104*, 11708.
- [40] K. Mallik, M. Mandal, N. Pradhan, T. Pal, *Nano Lett.* **2001**, *1*, 319.
- [41] L. H. Lu, H. S. Wang, Y. H. Zhou, S. Q. Xi, H. J. Zhang, J. W. Hu, B. Zhao, *Chem. Commun.* **2002**, 144.
- [42] J. P. Wilcoxon, P. P. Provencio, *J. Am. Chem. Soc.* **2004**, *126*, 6402.
- [43] P. R. Selvakannan, A. Swami, D. Srisathiyarayanan, P. S. Shirude, R. Pasricha, A. B. Mandale, M. Sastry, *Langmuir* **2004**, *20*, 7825.
- [44] S. P. Chandran, J. Ghatak, P. V. Satyam, M. Sastry, *J. Colloid Interface Sci.* **2007**, *312*, 498.
- [45] J. Zhang, Y. Tang, L. Weng, M. Ouyang, *Nano Lett.* **2009**, *9*, 4061.
- [46] M. Moskovits, I. Srnová-Šloufová, B. Vičková, *J. Chem. Phys.* **2002**, *116*, 10435.
- [47] J. Yang, J. Y. Lee, H. P. Too, *J. Phys. Chem. B* **2005**, *109*, 19208.
- [48] Z. Y. Li, J. Yuan, Y. Chen, R. E. Palmer, J. P. Wilcoxon, *Appl. Phys. Lett.* **2005**, *87*, 243103.
- [49] X. M. Lin, C. M. Sorensen, K. J. Klabunde, *J. Nanopart. Res.* **2000**, *2*, 157.
- [50] N. Goubet, Y. Ding, M. Brust, Z. L. Wang, M. P. Pileni, *ACS Nano* **2009**, *3*, 3622.
- [51] Q. B. Zhang, J. P. Xie, J. H. Yang, J. Y. Lee, *ACS Nano* **2009**, *3*, 139.
- [52] A. B. Smetana, K. J. Klabunde, C. M. Sorensen, A. A. Ponce, B. Mwale, *J. Phys. Chem. B* **2006**, *110*, 2155.
- [53] D. K. Lee, N. M. Hwang, *Scr. Mater.* **2009**, *61*, 304.
- [54] Y. Yang, Y. Yan, W. Wang, J. R. Li, *Nanotechnology* **2008**, *19*, 175603.
- [55] B. L. V. Prasad, S. I. Stoeva, C. M. Sorensen, K. J. Klabunde, *Chem. Mater.* **2003**, *15*, 935.
- [56] H. Hiramatsu, F. E. Osterloh, *Chem. Mater.* **2004**, *16*, 2509.
- [57] K. M. Nam, J. H. Shim, H. Ki, S. I. Choi, G. Lee, J. K. Jang, Y. Jo, M. H. Jung, H. Song, J. T. Park, *Angew. Chem., Int. Ed.* **2008**, *47*, 9504.
- [58] Z. Yang, K. J. Klabunde, *J. Organomet. Chem.* **2009**, *694*, 1016.
- [59] Z. C. Xu, C. M. Shen, Y. L. Hou, H. J. Gao, S. H. Sun, *Chem. Mater.* **2009**, *21*, 1778.
- [60] C. Voisin, N. Del Fatti, D. Christofilos, F. Vallée, *J. Phys. Chem. B* **2001**, *105*, 2264.
- [61] I. Lee, S. W. Han, K. Kim, *Chem. Commun.* **2001**, 1782.
- [62] P. B. Johnson, R. W. Christy, *Phys. Rev. B* **1972**, *6*, 4370.
- [63] X. Wang, Z. Y. Zhang, G. V. Hartland, *J. Phys. Chem. B* **2005**, *109*, 20324.
- [64] W. S. Rasband, ImageJ, Version 1.38x (available from <http://rsb.info.nih.gov/ij/>), National Institutes of Health, Bethesda, MD, 2009 (accessed February 2010).
- [65] C. F. Bohren, D. R. Huffman, *Absorption and Scattering of Light by Small Particles*, Wiley, New York **1983**.
- [66] M. Debenham, G. D. Dew, *J. Phys. E: Sci. Instrum.* **1981**, *14*, 544.

Received: July 7, 2010
Revised: October 25, 2010
Published online: